Sediment dynamics during the rainy season in tropical highland catchments of central Mexico using fallout radionuclides

Olivier Evrard[a *], Julien Némery[b], Nicolas Gratiot[b], Clément Duvert[b], Sophie Ayrault[a], Irène Lefèvre[a], Jérôme Poulenard[c], Christian Prat[b], Philippe Bonté[a], Michel Esteves[b]

[a] Laboratoire des Sciences du Climat et de l'Environnement (LSCE/IPSL) – Unité Mixte de Recherche 8212 (CEA, CNRS, UVSQ), 91198-Gif-sur-Yvette Cedex, France

[b]Laboratoire d'étude des Transferts en Hydrologie et Environnement (LTHE) – (IRD, G-INP, Université de Grenoble 1, CNRS), BP 53, 38041-Grenoble Cedex 9, France

[c]Université de Savoie, Centre Alpin de Recherche sur les Réseaux Trophiques des Écosystèmes Limniques (CARRTEL), Savoie Technolac, 73376-Le Bourget du Lac, France

* Corresponding author. Tel. +33/1/69.82.35.20 ; e-mail: olivier.evrard@lsce.ipsl.fr.

Abstract

Tropical regions are affected by intense soil erosion associated with deforestation, overgrazing, and cropping intensification. This land degradation leads to important on-site (e.g., decrease in soil fertility) and off-site (e.g., reservoir siltation, water pollution) impacts. This study determined the mean soil particle and sediment residence times in soils and rivers of three subcatchments (3–12 km^2) with contrasted land uses (i.e., cropland, forests, rangelands) draining to a reservoir located in highlands of the transvolcanic Mexican belt. Calculations were based on rainfall amount and river discharges as well as on fallout radionuclide measurements (Be-7, Cs-137, Pb-210) conducted on rainfall precipitated samples, soil sampled in the catchments, and suspended sediment collected by automatic samplers in the river during most storms recorded throughout the 2009 rainy season. Calculations using a radionuclide two-box balance model showed that the mean residence time of sediment in soils ranged between 5000±1500 and 23,300±7000 years. In contrast, sediment residence time in rivers was much shorter, fluctuating between 50±30 and 200±70 days. The shortest mean

residence times were measured in a hilly catchment dominated by cropland and rangelands, whereas they were the longest in an undulating catchment dominated by forests and cropland. Calculation of the Be-7/excess-Pb-210 in both rainfall and sediment allowed gaining insight on sediment dynamics throughout the rainy season. The first heavy storms of the year exported the bulk of the sediment stock accumulated in the river channel during the previous year. Then, during the rainy season, the two steeper catchments dominated by cropland and rangelands reacted strongly to rainfall. Sediment was indeed eroded and exported from both catchments during single heavy storms on several occasions in 2009. In contrast, the agro-forested catchment with gentler slopes exported sediment at a constant and low rate throughout the rainy season. Overall, land cover and flood type clearly proved to exert more control on sediment export than slope steepness and rainfall erosivity. Our results show the priority of stabilising old gully systems to prevent their extension by regressive erosion to cropland and to concentrate the implementation of on-site erosion control measures in cropland and rangeland of the most reactive catchments.

Keywords: tropical environments; erosion; suspended sediment; residence time; fallout radionuclides.

1.Introduction

Land degradation is particularly severe in tropical regions, such as in Mexico (Descroix et al., 2008), in southern China (Barton et al., 2004) or in eastern Africa (Nyssen et al., 2004). In these regions, overgrazing, deforestation, and intensification of food crop cultivation have led to severe erosion and to a decline in soil fertility (Roldán et al., 2003). Furthermore, once it reaches the river, sediment leads to numerous problems in downstream areas (Owens et al., 2005). It causes, for instance, an increase in water turbidity and a rapid filling of reservoirs. Sediment is also associated with numerous substances and contaminants (e.g., metals, nutrients, organic compounds, antibiotics; e.g., Tamtam et al., 2008; Le Cloarec et al., 2009).

These chemicals can then be bioaccumulated by organisms such as fishes ingesting particles and they can lead to public health problems after their consumption (e.g., Sánchez-Chardi et al., 2009; Urban et al., 2009). In mountainous environments, the problems associated with sedimentation are exacerbated by the important quantities of sediment produced during storms (e.g., Meybeck et al., 2003; Mano et al., 2009).

Sediment supply to the river needs to be controlled to prevent these problems. However, the main erosion sources fist need to be determined and the transit times of sediment within rivers need to be evaluated to implement appropriate and effective erosion control measures. In mountainous areas, the transit of sediments within rivers is affected by their specific flow regime (e.g., Dedkov and Moszherin, 1992). In tropical areas where hydrology is controlled by the succession of a dry and a rainy season, we generally assume that the increase in discharge at the beginning of the rainy season leads to an important resuspension of sediment accumulated in the river channel (e.g., Susperregui et al., 2009). However, the dynamics of this resuspension process and its implications on the sediment transit within ephemeral rivers throughout the rainy season are poorly understood.

The use of radionuclides with different half lives (i.e., Be-7, Cs-137, and excess-Pb-210) can contribute to investigate this issue. Dominik et al. (1987) designed a model to estimate the residence time of sediment within the Rhône River using these radionuclides. Bonniwell et al. (1999) proposed another methodology based on the Be-7/excess-Pb-210 ratio to estimate residence times and transport distances of sediment in a catchment dominated by snowmelt hydrology. They also applied this method in several catchments located in northern United States (e.g., Wilson et al., 2005). Matisoff et al. (2005) proposed, for instance, to calculate an indicator of the suspended sediment age by conducting this Be-7/excess-Pb-210 ratio based on radionuclide measurements conducted on both rainfall and suspended sediment samples. More recently, Le Cloarec et al. (2007) improved the partly indeterminate two-box

model proposed by Dominik et al. (1987) by taking account of the contribution of the dissolved radionuclide fraction to the river fluxes and by introducing the Cs-137 inventory in soils as an additional constraint, allowing to solve the system of radionuclide mass balance equations. These model improvements allowed calculating sediment residence times in the Seine River lowland basin in France.

However, to our knowledge, this methodology has never been implemented in catchments located under the tropics. Previous studies estimating radionuclide fluxes generally outlined the necessity to conduct a continuous monitoring of discharge and sediment concentration in rivers to strengthen the reliability of their results (e.g., Bonniwell et al., 1999; Le Cloarec et al., 2007). We therefore combine the use of continuous monitoring techniques (i.e., the installation of river gauging stations and automatic sediment samplers in several subcatchments of a larger mountainous catchment) and the measurement of fallout radionuclides in both rainfall and suspended sediment samples to quantify sediment residence times in a tropical highland region of central Mexico. This region concentrates the major part of the country's population (INEGI, 2006). We conducted this study in subcatchments representative of potential sediment sources areas draining to a reservoir that provides 25% of water distributed to Morelia city (ca. 1,000,000 inhabitants). We will use the two-box model improved by Le Cloarec et al. (2007) to calculate the mean soil particle and sediment residence times in those tropical subcatchments characterised by the succession of a rainy season and a (long) dry season. The indicator of suspended sediment age proposed by Matisoff et al. (2005) will also be calculated to outline the intra-annual sediment dynamics within those subcatchments. Finally, the implications of these findings for soil conservation in tropical highlands will be discussed.

2. Materials and methods

105

106 *2.1. Study area*

107

108 The Cointzio catchment covers an area of 630 km^2 located in the transverse volcanic
109 belt of central Mexico (Fig. 1). The catchment bedrock consists of igneous rocks generated by
110 Quaternary volcanic activities. According to the World Reference Base for soil resources
111 (FAO, 2006), soils within the catchment are mainly Acrisols on the hillslides, Andisols and
112 Cambisols in headwater areas, and Luvisols in the plains (INEGI, 1985). The Cointzio
113 catchment undergoes temperate subhumid climate conditions, according to the Köppen
114 climate classification system. In this region, rainfall mostly occurs between May and October.
115 The river network, which is mostly ephemeral, is dominated by the Rio Grande de Morelia
116 River. A dam is located at the outlet of the catchment, 13 km upstream of Morelia city (ca.
117 1,000,000 inhabitants). This dam was built in 1940 to supply water for domestic consumption
118 as well as for industrial and agricultural activities. The Cointzio reservoir (6 km^2; 65×10^6 m^3)
119 undergoes significant sedimentation, which leads to an increase in water turbidity in the lake
120 inducing a drastic decline in the zooplankton population disturbing the entire trophic chain
121 (Ramirez-Olvera et al., 2004) and to a 20% loss of its water storage capacity (Susperregui et
122 al., 2009). Increasing siltation of this reservoir is a major concern in the Morelia region where
123 it supplies a significant part of distributed water.

124 In 1975, forests occupied ca. 25% of the catchment surface. Then, after a period of
125 deforestation (1986–1996), a significant part of the cut areas recovered, and forests were
126 observed on ca. 30% of the Cointzio catchment area in 2003 (López-Granados et al., 2001;
127 Mendoza and López-Granados, 2007). Soil erosion within the catchment is mainly restricted
128 to the mountain piedmonts (Servenay and Prat, 2003). Concentrated erosion leading to the
129 formation of long and deep gullies is mainly observed on Acrisols. In contrast, Andisols and

Cambisols, which are also known to be sensitive to erosion (Poulenard et al., 2001), are mostly affected by sheet erosion (Bravo-Espinoza et al., 2009). In areas confronted with severe erosion, soil was completely removed, leading to the exposition of igneous weathered rocks and tuffs (locally referred to as "tepetates") at the ground surface (Etchevers Barra et al., 2004).

Three subcatchments (i.e., Huertitas, La Cortina, Potrerillos) representative of the different potential sources areas supplying sediment to the Cointzio reservoir were monitored in the framework of the DESIRE (Desertification mitigation and remediation land – A global approach for local solutions) and STREAMS (*Sediment TRansport and Erosion Across Mountains*) projects (Fig. 1). These subcatchments are characterised by different land uses, slope gradients, and soil conditions in order to cover the range of environments found in the Cointzio catchment (Fig. 2; Table 1). Each of them is drained by a deep (2–4 m) and narrow (1–5 m) river channel. Riverbed material is fine-sized (clay to sand-sized) and river banks are extensively colonized by seeds and shrubs increasing their cohesion and preventing their collapse.

Huertitas (3 km^2) consists of Acrisols covered by cropland and rangeland. It is characterised by a hilly topography, and 6% of its surface is affected by severe soil erosion (i.e., gullies and small ephemeral rills; Fig. 3). Some small-scale landslides occur sometimes in steep rangeland terrains. Land use in La Cortina (9 km^2) is dominated by pine-oak forests (i.e., *Quercus rugosa* and *Pinus montezumae*) and cropland located on undulating hillslopes underlain by Andisols. Finally, the rolling subcatchment of Potrerillos (12 km^2) is underlain by Acrisols and Andisols and is covered by almost equivalent proportions of pine-oak forests and eucalyptus plantations, cropland, and rangeland (Fig. 2C). Gullies only affect 1% of its surface (Table 1). The contribution of those potential sediment sources areas to the Cointzio

reservoir siltation and the rate at which sediment transfer operates is a subject of intense debate for the population living in the Morelia region.

2.2. Field measurements

2.2.1. Rainfall and discharge

Rain gauges and river monitoring stations were installed at the outlet of the three subcatchments (Fig. 1). They provided continuous precipitation and water discharge data derived from continuous water level measurements (with a 5-min time step) obtained with a Thalimede OTT water level gauge, stored by a data logger device (Campbell CR800), and corrected using stage-discharge rating curves (see Duvert et al., in press, for details on this method). Given that rainfall kinetic energy is often used as an indicator of rainfall erosivity, kinetic energy (*KE*; J m^{-2}) of each rainfall event was calculated using Eq. (1) (Salles et al., 2002):

$$KE_{mm} = \sum_i 8.95 + 8.44(\log_{10} I_i) \quad (1)$$

where KE_{mm} is the volume-specific kinetic energy (J m^{-2} mm^{-1}), and *I* is the rainfall intensity at the five-min time step (mm h^{-1}).

Rainfall was collected during 13 storms throughout the 2009 rainy season in a graduated PVC container located at the outlet of the Cointzio catchment to determine its content in Be-7 and Pb-210. We poured HCl (1.2 N) into the container to prevent radionuclide sorption on its sides. After each rain, water volume was measured in the container. Then, dissolved $AlCl_3$ (~ 5 g) was added to the rainfall sample within the few days following the storm and shaken for 1 h (Ciffroy et al., 2003). Pouring of NaOH to reach a pH of 8–9 precipitated the dissolved Al, carrying Be-7 and Pb-210 with a recovery efficiency between 80 and 95% (Ciffroy et al., 2003). Samples were filtered, air-dried, and sent to France for

179 radionuclide analysis.

180

181 *2.2.2. Measurement of SSC*

182

183 At the outlet of each subcatchment, data on suspended sediment concentration (SSC; g
184 L^{-1}) were obtained using an automatic water sampler (ISCO 3700) triggered by water level
185 variations. During floods, water samples were collected after each 5-cm water level variation.
186 This sampling frequency was selected based on the mean characteristics (i.e., flood duration,
187 shape of rising and falling limbs) of the floods recorded previously (i.e., between 2006 and
188 2008; Duvert and Gratiot, unpublished data) in the subcatchments to obtain a trade-off
189 between a satisfactory event coverage and a reasonable amount of samples to collect in the
190 field (see Duvert et al., in press, for details).

191 SSC of each sample (generally ≥ 2 g L^{-1}) was estimated in laboratory by weighing an
192 aliquot of ca. 200 ml after drying it for 24 h at 60°C. For each flood, a composite sample was
193 prepared by mixing all the available individual samples. This allowed obtaining a mean
194 representative sample of each individual flood with a quantity of fine sediment (2–50 g)
195 sufficient to conduct radionuclide analyses.

196 Instantaneous suspended sediment flux SSF (t s^{-1}) was then calculated using Eq. (2):

197 $$SSF = Q \cdot SSC \cdot 10^{-3} \quad (2)$$

198

199 Suspended sediment yield (SSY; in ton, t) was also calculated for each flood using Eq. (3):

200 $$SSY = \int_{t_0}^{t_f} SSF \; dt \quad (3)$$

with t_0 and t_f corresponding to the beginning and the end of the storm considered, between May and November 2009. In total, 89 events that occurred between May and November 2009 were sampled at the outlet of the three subcatchments.

2.2.3. Soil collection

Soils representative of the different land uses observed in the three subcatchments were collected. Sampling was concentrated in potential sediment source areas. For each potential source, we collected five samples of surface material (top 2–5 cm) and mixed them well to provide a homogeneous sample. In total, 30 representative samples were collected in the field between June and November 2009 (Fig. 1).

2.3. Radionuclide analysis

2.3.1. Radionuclides of interest

Be-7 is a natural cosmogenic radionuclide generated in the stratosphere and the upper troposphere. Most Be-7 reaches the ground surface as wet fallout. It is strongly fixed to the particles and mostly remains at the soil surface (i.e., in the uppermost 2 cm of the soil). Given its short half-life ($T_{1/2}$ = 53 d), it is used to document soil erosion over the short term (e.g., Sepulveda et al., 2008).

Pb-210 is a natural radionuclide ($T_{1/2}$ = 22.3 y), which is a decay product of U-238 ($T_{1/2}$ = 4.5 10^9 y). U-238 decays through a series of short-lived nuclides (e.g., Ra-226, Ra-222). Ra-222 is a gas that partly remains *in situ*, forming "supported" Pb-210; and it partly

escapes to the atmosphere, forming "excess" Pb-210, when falling back on the soil surface by wet and dry fallout. It then strongly sorbs to soil particles.

Cs-137 is an artificial radionuclide ($T_{1/2}$ = 30 y) produced by the thermonuclear bomb testings conducted during the 1960s as well as, in certain regions of the world (i.e., mainly in Europe), by the Chernobyl accident in 1986. It is now stored in soils, and this Cs-137 stock decreases by radioactive decay and by fine sediment transfer to the rivers.

Those three radionuclides are characterised by high K_d partition coefficients (e.g., Wang and Cornett, 1993; Gil-Garcia et al., 2009) and allowed therefore to trace sediment within catchments. The behaviour of those three radionuclides during sediment transport is further discussed in Le Cloarec et al. (2007).

2.3.2. Rainfall sample analysis

Precipitated rainfall samples were placed in polypropylene tubes. Counting was conducted at the *Laboratoire des Sciences du Climat et de l'Environnement* (LSCE) in Gif-sur-Yvette (France) using a low-background, high-efficiency, well-type Ge detector with a crystal volume of 220 cm^3 (GWL-220-15 Ortec). All samples were analysed within < 53 d (corresponding to the Be-7 half life) after the rainfall event. Counting time reached ca. 1×10^5 s to minimise the associated errors (typically 10–30% for Be-7).

2.3.3. Soil and sediment analysis

Soil and composite suspended sediment samples were packed into 15- or 60-ml (depending on the sediment quantity available in collected runoff) pre-tared polyethylene specimen cups and sealed airtight to contain Rn-222 and allow ingrowth of its decay products.

Be-7 (477.6 keV), Cs-137 (661.6 keV), and Pb-210 (46.5 keV) activities in this sediment were determined by gamma spectrometry using the seven very low-background coaxial N- and P-types GeHP detectors (Canberra / Ortec) available at the LSCE. "Excess" Pb-210 was calculated by subtracting the supported activity (determined using two U-238 daughters, i.e. Pb-214, by taking the average count number at 295.2 and 351.9 keV, and Bi-214 at 609.3 keV) from the total activity of Pb-210 (measured at 46.5 keV; Le Cloarec et al., in press).

When material available was insufficient (< 5 g), suspended sediment samples were placed in polypropylene tubes, sealed airtight, and counted on the well-type Ge detector used for rainfall precipitated sample analysis. Counting time of soil and sediment samples varied between 8×10^4 and 3×10^5 s to limit errors on activity determination (typically 5–10% except for Be-7 with ca. 10–30%) and for practical reasons (i.e., to allow counting one sample d^{-1} on each detector). All measured counts were corrected for background levels measured at least every 2 months as well as for detector and geometry efficiencies. Results were systematically expressed in Bq kg^{-1}. Radionuclide activities were systematically corrected according to the decay after the sampling period. Counting efficiencies and quality insurance were conducted using internal and certified IAEA standards (i.e., IAEA-135, IAEA-375, IAEA-CU-2006-03, IAEA-Soil-6, RGU-1, RGTh-1) prepared in the same specimen cups as the samples. Efficiencies were interpolated for Be-7 energy.

To obtain information on the grain size of sediment, scandium was analysed by Instrumental Neutron Activation Analysis (INAA). Concentration in this trace element is widely used as a proxy of the fine grain size fraction of sediment (e.g., Jin et al., 2006; Dias and Prudêncio, 2008). Dried sediment subsamples (ca. 40–80 mg) were packed into tightly closed plastic bags, without any preliminary digestion. The subsamples were exposed to irradiation in the experimental nuclear reactor Orphée at the Commissariat à l'Energie Atomique (CEA; Saclay, France). The subsamples underwent a flux of thermal neutrons of

275 2.13 10^{13} n cm^{-2} s^{-1} during 30 minutes. After a 4-days cooling, four successive measurements
276 of gamma activities were carried out using HPGe detectors. Two reference materials (i.e.,
277 IAEA SL-1 and Soil-7) were systematically used to cross-check the results. The uncertainty
278 on these measurements is ≤ 5%.
279
280 *2.4. Calculating the radionuclide and sediment catchment budget*
281 This work is based on a simple hypothesis stating that measuring the fallout input and
282 the river output of radionuclides characterised by very high K_d values at the catchment scale
283 allows tracing particles that adsorb those radionuclides (section 2.4.1). In a second step, the
284 construction of a radionuclide catchment budget then provides a way to estimate the residence
285 time of radionuclides and particles/sediment within the catchment (section 2.4.2).
286
287 *2.4.1. Calculating the radionuclide and sediment input and output fluxes*
288 Atmospheric deposition of Be-7 and Pb-210 was estimated based on the analysis of
289 the rainfall precipitated samples, by multiplying the precipitate activity (Bq L^{-1}) by the
290 corresponding rainfall amount (L m^{-2}). Samples were collected all throughout the rainy season
291 in order to take account of the temporal variations of the radionuclide flux. Atmospheric Cs-
292 137 flux is currently considered as undetectable.
293 The mean radionuclide river fluxes (C) from each subcatchment were then calculated
294 using Eq. (4):

295 $$C = C_{SM} \times (SSC + \frac{1}{K_d}) \quad (4)$$

296 where C_{SM} is the radionuclide activity per mass of dry matter (Bq kg^{-1}), SSC is the suspended sediment
297 concentration (kg L^{-1}), and K_d is the distribution coefficient between particular and dissolved phases (L
298 kg^{-1}).

299 K_d values for the different radionuclides were discussed by Le Cloarec et al. (2007)
300 who decided to use the following values: 8.4×10^4 for Cs-137, 5×10^4 for Pb-210, and 10×10^4
301 for Be-7.
302
303 *2.4.2. Modelling the sediment residence times*
304 After constructing simple one-box radionuclide balance models using Cs-137 or Pb-
305 210 to estimate the residence time of radionuclides and sediment in the upstream part of the
306 Rhône River catchment (Switzerland), Dominik et al. (1987) proposed to integrate Be-7 into
307 this model to benefit from potential additional information provided by this radionuclide on
308 the rapid delivery of sediment to the river. However, because of its short half-life, the bulk of
309 Be-7 would decay in the soil of the catchment before reaching the river. To overcome this
310 problem, Dominik et al. (1987) developed a two-box balance model. The catchment surface
311 was then subdivided into two boxes: (i) a "soil-box" (which is referred to by an *s* subscript in
312 the remainder of the text and equations) characterised by an S_s-area, low transport velocities
313 and hence long radionuclide residence times (the soil box comprises the uppermost soil
314 surface submitted to radionuclide fallout) and (ii) a "river-box" (which is referred to by an *r*
315 subscript in the remainder of the text and equations) covering the river area and its
316 surroundings (S_r) characterised by faster exchanges and shorter radionuclide residence times.
317 Input and output fluxes of sediment and radionuclides were taken into account in each box.
318 Radioactive decay during the residence time of sediment was also considered. The initial
319 version of the model hypothesised that radionuclides were exclusively transported on soil
320 particles, whereas the version developed by Le Cloarec et al. (2007) takes into account the
321 radionuclide dissolved fractions transported in the river using the K_d values.
322 Total atmospheric input fluxes (F_a) were estimated based on the rainfall precipitated
323 samples, and the fraction present in each box was also determined (Eq. 5):

$$S_r + S_s = 1 \quad (5)$$

Mass balance equations were calculated for each reservoir. In the soil box, loss of material is due to material transfer to the river box or to radioactive decay (Eq. 6):

$$F_a \times S_s = I_s \times (k_s + \lambda) \quad (6)$$

where k_s is the rate of output transfer from the soil box (related to the residence time τ_s in the box, with $k_s = 1 / \tau_s$); I_s is the radionuclide inventory in the soil box; and λ is the constant of radioactive decay.

In the river box, atmospheric inputs were added to the flux coming from the soil box. Both fluxes were required to balance the output from the river and the radioactive decay (Eq. 7):

$$F_a \times S_s + I_s \times k_s = I_r \times (k_r + \lambda) \quad (7)$$

where I_r is the radionuclide inventory in the river box and k_r is the rate of output transfer from the river box.

The flux exported from the river box (F_r) was then calculated using Eq. (8).

$$F_r = I_r \times k_r \quad (8)$$

In the initial version of the model (Dominik et al., 1987), Eqs. (5) to (8) were only calculated for Be-7 and excess-Pb-210. In the version adapted by Le Cloarec et al. (2007), additional equations were introduced for Cs-137. This simultaneous use of the three radionuclides allowed solving the system of equations.

For each radionuclide, five variables had to be determined (S_r, k_r, k_s, I_s, and I_r). Additional assumptions were necessary to solve Eqs. (5) to (8). They were based on the comparison between λ–values and the expected k_s and k_r values. First, we hypothesised that the residence time in the soil box was expected to be an order of magnitude of decades to centuries. Most Be-7 ($T_{1/2}$ = 53 d) will therefore be lost by decay and its export from the soil

box was considered as negligible compared to atmospheric fluxes ($k_s << \lambda_{Be}$ and $(I_s)_{Be} \times k_s << S_r \times (F_a)_{Be}$). Second, export of material from the river box was expected to remain in the same order of magnitude as the residence time of sediment within the river, which is significantly more rapid than the decay of excess-Pb-210. Decay of this radionuclide could therefore be neglected ($\lambda_{Pb} << k_r$).

A relationship between the river box area (S_r) and the associated removal rate of material (k_r) could be derived based on the assumption on Be-7 and by combining Eqs. (7) and (8):

$$S_r = \left(\frac{F_r}{F_a}\right)_{Be} \times \left(\frac{\lambda_{Be}}{k_r + 1}\right) \quad (9)$$

Based on the hypothesis for excess-Pb-210 and combining the mass balance equations of Be-7 and excess-Pb-210, the residence time of sediment could be determined (Eq. 10):

$$\tau_s = \frac{\left(\frac{1}{\lambda_{Pb}}\right) \times \left[1 - \left(F_a / F_r\right)_{Pb}\right]}{\left(R_r / R_a\right) \times \left(1 + \lambda_{Be} \times \tau_r\right) - 1} \quad (10)$$

where $R_r = \frac{\left(F_r\right)_{Be}}{\left(F_r\right)_{Pb}}$ and $R_a = \frac{\left(F_a\right)_{Be}}{\left(F_a\right)_{Pb}}$

Another relationship implicating τ_s and τ_r was derived from the mass balance equations of Cs-137. Given the atmospheric flux of Cs-137 is currently negligible ($\left(F_a\right)_{Cs} = 0$), its inventory in soils is well known (total inventory of 1130 (± 250) Bq m^{-2} according to measurements carried out in 2009 in the study sites). Based on Eq. (7), we could then determine τ_s (Eq. 11):

$$\tau_s = \frac{\left[M - \left(F_r\right)_{Cs} \times \tau_r\right]}{\left(F_r\right)_{Cs} \times \left(\lambda_{Cs} \times \tau_r + 1\right)} \quad (11)$$

with $M = \left(I_s\right)_{Cs} + \left(I_r\right)_{Cs}$

Finally, the combination of Eqs. (10) and (11) allowed for determining τ_r (Eq. 12):

$$a(\tau_r)^2 + b(\tau_r) + c = 0 \quad (12)$$

with

$$a = -(F_r)_{Cs} \times \left(\frac{R_r}{R_a}\right) \times \lambda_{Be} \times \lambda_{Pb}$$

$$b = M \times \left(\frac{R_r}{R_a}\right) \times \lambda_{Be} \times \lambda_{Pb} - (F_r)_{Cs} \times \lambda_{Pb} \times \left[\frac{(R_r)}{(R_a)} - 1\right] - (F_r)_{Cs} \times A \times \lambda_{Cs}$$

$$c = \lambda_{Pb} \times M \times \left[\frac{R_r}{R_a} - 1\right] - A \times (F_r)_{Cs} \times A = 1 - \left(\frac{F_a}{F_r}\right)_{Pb}$$

A sensitivity analysis of the model was carried out by Le Cloarec et al. (2007). They showed that the major uncertainty was the one associated with SSC measurements. In this study, this uncertainty reached 15 to 30% (Némery et al., 2010). Overall, the uncertainties on soil particle and sediment residence times provided by the model were estimated at 30%.

2.6. Estimation of suspended sediment age and fraction of new sediment

The methodology proposed by Matisoff et al. (2005) was followed to determine the age of sediment (*t*; Eq. 13) and the percentage of "new" suspended sediment in the river (Eq. 14):

$$t = \frac{-1}{(\lambda_{7Be} - \lambda_{210Pb})} \ln\left(\frac{A}{B}\right) + \frac{1}{(\lambda_{7Be} - \lambda_{210Pb})} \ln\left(\frac{A_0}{B_0}\right) \quad (13)$$

where λ_{7Be} and λ_{210Pb} are the decay constants of ^{7}Be and ^{210}Pb (d^{-1}); A and B are the ^{7}Be and $^{210}Pb_{xs}$ activities in the suspended sediment (Bq kg^{-1}); A_0 and B_0 are the ^{7}Be and $^{210}Pb_{xs}$ activities in rainfall (Bq L^{-1}).

$$\%\text{ of "new" sediment } = 100 \times \frac{(A/B)}{(A_0/B_0)} \quad (14)$$

Both parameters were calculated for all the floods sampled in the three study sites throughout the 2009 rainy season. This second approach was hence simpler than the two-box model. A decrease in the Be-7/excess-Pb-210 ratio can then alternatively be explained by (i) an increase in the sediment residence time (given Be-7 decay is faster than excess-Pb-210 decay) or by (ii) the dilution of sediment enriched in Be-7 by sediment poorer in Be-7. Consequently, calculation of this ratio does not theoretically allow deciding whether aging or dilution of sediment occurred in the river.

3. Results and discussion

3.1. Main runoff and erosion trends during the 2009 rainy season

Overall, the total rainfall depth measured in the monitored subcatchments during the 2009 rainy season can be considered as "normal" (593–1169 mm) compared to the long-term (1954–2004) rainfall database (400–1100 mm yr^{-1}) available for Santiago Undameo, located just upstream of the Cointzio reservoir (Gratiot et al., 2010). Rainfall amount strongly varied from one subcatchment to another. La Cortina received much more rainfall (1169 mm) than Potrerillos (765 mm) and Huertitas (593 mm). Furthermore, two storms that occurred in June 2009 were unrecorded in Huertitas because of technical problems. This partly explains the lower rainfall amount recorded in Huertitas compared to the two other subcatchments. Most of the recorded events consisted of heavy storms associated with vertical convective cloud systems and characterised by rainfall intensities reaching up to 120 mm h^{-1} in 5 min. Mean rainfall erosivity was more than twofold higher in La Cortina (mean of 434 J m^{-2} mm^{-1} during the season) than in Potrerillos (204 J m^{-2} mm^{-1}) and Huertitas (214 J m^{-2} mm^{-1}) (Table 2).

These storms generated variable runoff volumes in the three study areas. Runoff coefficients were extremely low in La Cortina (mean of 0.8%), except during the first significant storm of the year (3.9% on 14 July 2009). In contrast, mean runoff coefficients observed in Potrerillos and Huertitas were close to 7%, with higher coefficients observed during the heaviest storms (up to 14.0% in Huertitas and 17.8% in Potrerillos; Table 2). Furthermore, sediment export fluctuated strongly from one subcatchment to another. Overall, specific SSY was by far the most important in Huertitas (900–1500 t km^{-2} y^{-1}) and Potrerillos (600–800 t km^{-2} y^{-1}), whereas it was particularly low in La Cortina (30 t km^{-2} yr^{-1}; Duvert et al., in press). This major difference in erosion exports from the different subcatchments can be attributed to numerous factors. First, different land uses and soil types are observed in the different subcatchments (Fig. 2). A much higher proportion (52%) of the La Cortina subcatchment is indeed covered by forests, which are traditionally known to produce less sediment than grassland and cropland when they are not submitted to deforestation, logging, or frequent fires (e.g., Inbar et al., 1998; Prosser and Abernethy, 1999). Most soils in this subcatchment are Andisols, which are very permeable and generate less runoff than Acrisols. Furthermore, in cropland that covers 28–46% of the surface in the study sites, the bulk of erosion generally occurs when erosive storms fall on particularly erodible soils, which is typically the case at the beginning of the crop growing season (i.e., May-July). In 2009, 61–64% of total sediment export occurred during this period in La Cortina and Potrerillos, but only 46% in Huertitas (Table 2). This is probably due to the occurrence of particularly heavy storms in September in Huertitas (Table 2a).

Furthermore, SSY were higher in catchments with steeper slopes: 42% of the slopes in the Huertitas subcatchment are indeed ≥ 10°, compared to only 29% in Potrerillos and 21% in La Cortina (Table 1). The catchment size can also explain these SSY differences. In Potrerillos, the larger number of potential traps prevents sediment from reaching the river.

Collection of suspended sediment was carried out during most of the storms that occurred in 2009 (Table 2), corresponding to 77–87 % of the total sediment export from the different subcatchments (Duvert et al., in press). We can then confidently consider that our results are representative of the entire 2009 rainy season.

3.2. Radionuclide atmospheric fluxes

Atmospheric fluxes of radionuclides were considered as homogeneous in the Cointzio catchment, given that they are mainly controlled by latitudinal variations (e.g., Brost et al., 1991). A relationship between rainfall depth and radionuclide fallout could be derived for excess-Pb-210 and Be-7 (Fig. 5). A moderate to good correlation ($0.71 < R^2 < 0.76$, significant at $p < 0.005$) was found between rainfall and fallout radionuclides, which is consistent with the coefficients reported in the literature (e.g., Caillet et al., 2001). The linear relationship between radionuclide activity and precipitation (R; mm of rainfall) allowed calculating atmospheric Be-7 (Eq. 14) and excess-Pb-210 (in GBq km^{-2}; Eq. 15) depositions (Fig. 5).

$$\left(F_a\right)_{Be-7} = 10^{-3} \times \left(1.4R - 1.9\right) \qquad (R^2 = 0.71;\ p < 0.005) \qquad (14)$$

$$\left(F_a\right)_{xs-Pb-210} = 10^{-3} \times \left(0.09R - 0.4\right) \qquad (R^2 = 0.76;\ p < 0.005) \qquad (15)$$

La Cortina received the highest radionuclide atmospheric fluxes, which is explained by the higher rainfall depth measured in 2009 in this subcatchment (Table 3).

3.3. Radionuclide river fluxes

Total radionuclide river fluxes calculated by combining radionuclides fixed on sediment and dissolved radionuclides transported in the river water were found to be strongly

dependent on the suspended sediment concentration ($0.7 < R^2 < 0.8$ significant at $p < 0.001$; data not shown). The variation of these fluxes can hence be partly explained by strong SSC variations between the different subcatchments (Table 4). The lowest Be-7 and Pb-210 river fluxes were observed in La Cortina. In this subcatchment, the contribution of the atmospheric fluxes to the total radionuclide input was much more important than in the two other subcatchments (Table 4). Regarding Cs-137, the river flux was also the lowest in La Cortina.

3.4. Modelling the radionuclide content in sediment

To strengthen the results provided by the model, we must verify that the sediment particle size remained constant throughout the 2009 rainy season. Particle size, which could be estimated using the scandium concentrations as a proxy for the fine fraction present in sediment collected at the outlet of each subcatchment, was constant in 2009, as demonstrated by the low standard deviation observed around the mean scandium concentrations measured in sediment collected in La Cortina (22±1 ppm), Potrerillos (19±2 ppm) and Huertitas (21±1 ppm).

The model provided several useful insights over sediment residence times in the three subcatchments (Table 5).

The model calculated a mean residence time of sediment in both rapid and slow boxes. Mean residence time of soil particles in the slow box ranged between 5000 (± 1500) and 23,300 (± 7000) years. The longer residence time was calculated for La Cortina (23,300 ± 7000 years), whereas it was the shorter in Huertitas (5000 ± 1500 years). In Potrerillos, an intermediate residence time was calculated (13,300 ± 4000 years). These results were consistent with the slope characteristics and the intensity of erosion observed in these subcatchments (Table 1). Residence times were shorter in Huertitas, which is the steepest site

and the most affected by the development of deep gullies (Fig. 3). In contrast, residence times were the longest in the most forested site characterised by the gentlest slopes (i.e., La Cortina). Even though the surface of the monitored subcatchments remained in the same order of magnitude (3–12 km^2), the range of residence times in the soil boxes was as wide as the range calculated for different nested catchments within the entire Seine basin (between 4800 years in the first order catchments and up to 30,000 years in the entire Seine river basin; Le Cloarec et al., 2007). Soil erosion and its consequences on residence times of particles in soils were hence very variable in the three Mexican sites, which outlines their different hydrosedimentary behaviour. Within a few kilometres, erosion fluctuated indeed between low rates (30 t km^{-2} yr^{-1} in La Cortina) and particularly severe rates (900–1500 t km^{-2} y^{-1} in Huertitas).

Once it reached the river (i.e., rapid box of the model), sediment was rapidly exported from the subcatchments. This export occurred on average in less than one rainy season, with mean residence times of sediment in the river channel ranging between 50 (± 30) days in Potrerillos and 200 (± 70) days in La Cortina. The intermediate mean residence time estimated in Huertitas (60 ± 40 days) was not significantly different from the one calculated in Potrerillos. This residence time was highly dependent on the occurrence of heavy storms, leading to a significant proportion of the annual sediment yield. Mean residence times of sediment estimated in the Mexican rivers remained in the same order of magnitude as the ones measured in the Rhône mountainous basin (1–220 days; Dominik et al., 1987), whereas they were significantly shorter than the ones estimated in upstream rivers of the lowland Seine River basin (200–500 days; Le Cloarec et al., 2007).

The model also calculated the proportion of the subcatchment area belonging to the "rapid box", i.e., the river channel and the directly connected areas. This proportion reached 0.3±0.1% of the subcatchment surface in La Cortina where the river is located in a narrow (~

516 1 m) and incised channel flowing through forests and cropland. Despite a high rainfall amount
517 in 2009 (1169 mm), SSY from this subcatchment remained low (30 t km^{-2} y^{-1}); and the rapid
518 box was hence logically characterised by a small surface and rather long sediment residence
519 times (mean of 200 days compared to 50–60 days in the two other sites). Furthermore, the
520 absence of severely eroded areas in this subcatchment was confirmed by the very limited
521 surface of the rapid box calculated by the model.
522 In Potrerillos, the proportion covered by the rapid box was slightly higher (1.5±0.5%),
523 which is explained by the flowing of the river through a wider (2–5 m) channel across
524 rangeland, forests and cropland. In contrast, this surface proportion reached 4.5±1.5% in
525 Huertitas. This proportion of the subcatchment surface remained in the same order of
526 magnitude as the catchment proportion affected by severe erosion (6%). Hence, the model
527 associated the river bank gully systems, which are directly connected to the river, with the
528 rapid (i.e., river) box to evacuate all the sediment produced. Conceptually, we can indeed
529 reasonably consider that this gully surface sediment is rapidly transferred to the river, which
530 explains the different hydrosedimentary behaviour of the Huertitas subcatchment.
531 The particularly low content in Cs-137 (< 0.3 Bq kg^{-1}; Table 2) measured in several
532 samples collected at the outlet of Huertitas and Potrerillos led to model uncertainties specific
533 to regions with soils characterised by very low activities in Cs-137 (i.e., Mexico). Additional
534 measurements were therefore conducted on several suspended sediment samples using the
535 very low background, well-type gamma detectors available at the *Laboratoire Souterrain de*
536 *Modane* (Reyss et al., 1995). Overall, these results showed the presence of very low Cs-137
537 activities (0.2 ± 0.1 Bq kg^{-1}) in this sediment. To investigate uncertainties associated with
538 these very low activities, we attributed successively different Cs-137 activities (0, 0.1, and 0.2
539 Bq kg^{-1}) to the samples in which results were under the detection limits in Gif-sur-Yvette (i.e.,
540 typically < 0.3 Bq kg^{-1}) but detectable in Modane. The model results reported in Table 5 were

calculated using a Cs-137 activity of 0.2 Bq kg^{-1}. This change of the Cs activities mostly led to a ca. 15% variation of the particle residence times in the soil box. However, all variations affecting the model outputs systematically remained within the 30% model uncertainties mentioned above.

3.5. Suspended sediment age and fraction of "new" sediment

At the beginning of the rainy season, the rivers contained an important stock (74–88%) of older sediment deposited during the previous year (Fig. 6). This older sediment stock was progressively evacuated by the successive floods. Despite this feature common to the three study sites, two distinct hydrosedimentary behaviours could be outlined (Fig. 7).

In La Cortina, sediment export was mainly achieved by the first major flood of the rainy season (14 July; Fig. 6B). This storm was intense (438 J m^{-2} mm^{-1}) but not exceptional, given that rainfall intensity reached higher levels in La Cortina later during the season (up to 763 J m^{-2} mm^{-1} on 8 September; Table 2B). During this first storm, only 12±4% of new sediment were provided to the river. In contrast, this storm strongly contributed to the flush of the sediment accumulated in the river channel during the previous season. The supply of "new" sediment to the river remained continuous and stable during the rest of the season, regardless of storm erosivity (Fig. 6B). Only 11–21 % of "new" sediment were observed throughout the rainy season in the river channel of this site. Subsequent export of recent sediment from this forested subcatchment occurred at a rather constant and low rate (Fig. 7B). According to the calculation of the Be-7/excess-Pb-210, the mean residence time of sediment in the river channel reached 163±14 days. This value remained in the same order of magnitude as the one calculated by the radionuclide balance model (200±70 days; Table 5).

In contrast, in Huertitas and in Potrerillos, sediment residence time and the percentage of new sediment greatly fluctuated all throughout the rainy season. In Huertitas, sediment residence time in the river channel varied between 1 and 194 days. Evolution of this residence time displayed a sawtooth behaviour (Fig. 6A). For instance, the heavy storm that occurred on 3 September generated a dramatic supply of "new" sediment to the river (the proportion of new sediment in the river channel increased from 24±3% to 76±19%). This storm and the next events led to a complete flush of the river sediment stock and to the export of older sediments. Sediment residence times in the river dropped from 124±11 days to 38±37 days between 13 August and 4 September. Conceptually, this result means that, even though most sediment is gradually exported from Huertitas through a succession of deposition and resuspension steps, it can be exported from the catchment by a single heavy storm. The storm observed on 3 September was indeed the most intense of the year in Huertitas (487 J m^{-2} mm^{-1}; Table 2a). A similar fluctuating behaviour was observed in Potrerillos. Complete "sediment flush" of the river channel was observed twice in 2009 (on 17 August and 12 September; Fig. 6C). This sediment export was observed after particularly intense storms (> 200 J m^{-2} mm^{-1}; Table 2C). Overall, Huertitas and Potrerillos were characterised by much shorter sediment residence times in the river channel (111±42 days in Huertitas; 101±46 days in Potrerillos; Figs. 6A-C). This finding is consistent with the mean sediment residence time in the river calculated by the model (60±40 days in Huertitas; 50±30 days in Potrerillos; Table 5).

Regarding SSY, the first heavy storm of the rainy season — which traditionally coincides with a period characterised by a sparse cover of the soil by vegetation — led to the highest sediment export of the year. This was the case in the three monitored subcatchments. In contrast, during the rest of the season, Huertitas and Potrerillos were much more reactive than La Cortina (Fig. 7). Sediment stock in the river channel of these subcatchments was

hence successively renewed and evacuated during the rainy season. In contrast, La Cortina returned to a rather "dormant" hydrosedimentary behaviour after the first heavy storm of the season.

3.6. Radionuclide inventories

The model also provided the total radionuclide inventory in each "reservoir" (Table 6). The $(I_r/I_s)_{(Be)}$ ratio, which indicates that the Be-7 fraction originated from the atmosphere reached the river, was in the same order of magnitude as the proportion of the subcatchment surface belonging to the rapid (river) box (S_r; Table 5).

3.7. General discussion: control of flood type, rainfall erosivity and land use on sediment export and potential implications for soil conservation

We could not detect any clear effect of rainfall erosivity on sediment export. Overall, in 2009, heaviest storms occurred in La Cortina (KE_{mm} between 92 and 763 J m^{-2} mm^{-1}) but this higher erosivity was not reflected by higher SSY. The highest SSY were indeed observed in Huertitas and Potrerillos where rainfall was characterised by lower erosivities (58–520 J m^{-2} mm^{-1} in Huertitas and 42–463 J m^{-2} mm^{-1} in Potrerillos). Furthermore, high values of KE_{mm} were never associated with high SSC peaks in the three catchments. Duvert et al. (in press) conducted a factorial analysis on several parameters (e.g., flood type, antecedent moisture conditions, discharge, rainfall, etc.) collected in the three subcatchments to outline the driving factors of SSY. They showed that parameters associated with precipitation were absolutely not related to both sediment and discharge parameters, probably because of the

614 high spatial variability of rainfall. In contrast, peak discharge was significantly associated
615 with exported loads.
616 We can outline important insights on sediment dynamics in the river based on the
617 flood typology developed by Duvert et al. (in press). They classified the floods that we
618 analysed into three types: (i) events characterised by a lag between sediment peak and peak
619 discharge (referred to as "LaP" events); (ii) events characterised by the coincidence between
620 sediment peak and peak discharges (referred to as "SP" events) and (iii) events characterised
621 by a sediment peak leading the peak discharge (referred to as "LeP" events). Sediment
622 maintained high concentrations during the recession phase of those three flood types,
623 indicating that their export was rather "transport-limited" than "sediment-limited". Table 2
624 provides the typology attributed to each flood by Duvert et al. (in press). We could associate
625 those different flood types with indications on the sediment age and distinct hydrosedimentary
626 behaviours.
627 In Huertitas and in La Cortina, we only analysed one LaP flood. It corresponded to the
628 first significant flood of the rainy season (16 May in Huertitas, 14 July in La Cortina). This
629 flood refilled the river network with sediment and started flushing the sediment deposited in
630 2008 (74±4% of the flood export in Huertitas and 88±0.5% in La Cortina). This initial flush
631 was also associated with a limited export of sediment directly eroded from the hillslopes
632 (26±4% in Huertitas; 12±0.5% in La Cortina). In La Cortina, this event exported the bulk of
633 annual SSY, and was associated with the highest runoff coefficient of the season (3.9%). This
634 confirms the low sediment availability in the river draining this subcatchment. In Potrerillos,
635 LaP floods supplied recent sediment to the system. Proportion of "new" sediment increased
636 from 27±3% to 78±17% after these floods. In contrast, SP floods described as "overflow
637 waves" by Duvert et al. (in press) were associated with large runoff coefficients in Huertitas
638 and Potrerillos (4–16%) and exported a significant proportion of sediment in 2009 (37% of

639 SSY in Huertitas and even 77% in Potrerillos). The large dominance of SP floods (78%) in
640 Potrerillos illustrates the very reactive behaviour of this catchment. Finally, floods of LeP
641 type mostly evacuated the sediment stock available in the channel.
642 Given that sediment transport was rather "transport-limited" and that sediment
643 exhaustion was not detected in 2009, we can infer the important role played by land use on
644 sediment export. In the two subcatchments were gullies are found, they provided a constant
645 source of sediment to the river. This difference mostly explains the variation in sediment
646 export between Huertitas and Potrerillos — characterised by extensive gully networks — and
647 La Cortina.
648 Furthermore, although they were relatively low, Cs-137 activities measured in this
649 Mexican catchment were very contrasted, and they therefore allowed outlining the main
650 contributions of the different land uses to the sediment production (Table 7). In Huertitas, the
651 Cs activity associated with gullies was extremely low (0–0.2 Bq kg^{-1}), which can be explained
652 by the continuous export of fine sediment to the river since the Cs-137 deposition in the 1960s
653 and by the depletion of the Cs stock in these gully systems (Fig. 3). In contrast, a significant
654 Cs activity was measured in cropland (2.1 ± 0.3 Bq kg^{-1}). In Potrerillos, a similar Cs activity
655 was observed in cropland (2.2±0.3 Bq kg^{-1}), whereas rangeland was characterised by low —
656 but detectable — Cs concentrations (0.6±0.3 Bq kg^{-1}). Finally, Cs activities measured in La
657 Cortina were significantly higher than in the two other catchments, confirming the lower
658 depletion of the Cs stock by erosion. They fluctuated between 3.7±1.2 Bq kg^{-1} in cropland and
659 11.9±5.8 Bq kg^{-1} under forests.
660 We can compare activities measured in potential sediment sources with the ones
661 measured in suspended sediment at the outlet. In Huertitas, Cs-137 activities measured in
662 suspended sediment collected at the outlet were low (0.1–1.1 Bq kg^{-1}). These results
663 confirmed the limited contribution of upstream cropland to erosion. The bulk of sediment is

hence produced by the historical gully networks that grow by regressive erosion and that are characterised by low or very low Cs-137 activities. Gullies were probably formed due to the association of traditional cropping practices with cattle grazing on hillslopes. They are now partly stabilised but they keep extending by regressive erosion and conveying sediment from cropland to the river (Bravo-Espinoza et al., 2009). However, the higher contribution of upstream cropland to erosion cannot be excluded during heavy storms. This was typically the case at the beginning and at the end of the rainy season, when larger Cs activities were measured in sediment collected at the outlet and when higher runoff coefficients were observed (Table 2C).

In Potrerillos, low Cs-137 activities were also detected at the outlet, indicating that the contribution of cropland to erosion must remain limited. Contribution of cropland to erosion was also probably restricted to the most intense storms (e.g., on 11 September) or during the evacuation of sediment eroded by a succession of erosive storms (e.g., on 23 July; Table 2A).

In La Cortina, Cs-137 activities were clearly higher than at the outlet of the two other subcatchments. Cs-137 concentrations (mean values of 1–3.7 Bq kg^{-1}) remained in the same order of magnitude as the Cs-137 concentrations measured in samples collected from cropland in this subcatchment (mean values of 3.1–4.1 Bq kg^{-1}).

Obtaining an estimation of the sediment residence times in catchments and rivers is important to implement the appropriate conservation measures. Our results show that stabilising the historical gully systems observed in Huertitas should be a priority, given that they are characterised by much shorter residence times of sediment and that they produce the bulk of sediment exported from this subcatchment. They also keep growing by regressive erosion at the expense of cropland. In La Cortina, the major contribution of avocado and maize fields to erosion outlines the need to carry out on-site soil conservation measures. In Potrerillos, the limitation of cattle density could be envisaged to limit sediment export to the

river and to prevent the further extension of gullies to cropland. In this subcatchment, fine soil particles are indeed removed by cattle trampling, which leads to an increase in the surface of bare soils (Bravo-Espinoza et al., 2009).

5. Conclusions

This study combined for the first time the monitoring of suspended sediment transport in rivers and the measurement of fallout radionuclides (Be-7, Cs-137, excess-Pb-210) in rainfall, soil, and suspended sediment samples collected in three subcatchments representative of the environments draining to a reservoir located in tropical highlands of the transvolcanic Mexican belt. It provided a novel continuous hydrosedimentary monitoring of three contrasted catchments all throughout the rainy season. Soil particle residence time calculated by a radionuclide two-box balance model ranged between 5,000 (± 1,500) years in the 3 km^2 steeper catchment dominated by gully networks and cropland, and 23,300 (± 7,000) years in the 9-km^2 more gentle forested catchment. Once it reached the river, sediment was systematically exported from the catchments within a mean period ranging between 50 (± 30) and 200 (± 70) days. The first heavy storm of the rainy season led to the flush of sediment accumulated in the river channel during the previous season in the three study sites. Then, the flood type and the land use of the different subcatchments proved to control sediment export during the season. In a context of rapid siltation of the Cointzio reservoir that is crucial and strategic for the water supply in the region, the local authorities should concentrate their efforts to stabilise the gully systems, to prevent their extension by regressive erosion at the expense of cropland, and to encourage the implementation of conservation measures in cropland of the most reactive catchments (i.e., Huertitas, Potrerillos). Further research should now focus on fingerprinting and quantifying the contribution of the main sediment sources

714 within the most reactive catchments in order to outline the areas where the conservation
715 efforts and the limited subsidies available should be concentrated.
716
717 **Acknowledgements**
718 This is the LSCE contribution n°X. This work is a part of the STREAMS project, funded by
719 the French National Research Agency (ANR/ BLAN06-1_139157). It also benefited from
720 support of the DESIRE project co-funded by the European Union (UE6, Integrated project,
721 Contract N° 037046). The authors also wish to thank the two anonymous reviewers for their
722 useful comments on an earlier version of the manuscript.
723
724 **7. References**
725
726 Barton, A.P., Fullen, M.A., Mitchell, D.J., Hocking, T.J., Liguang Lou, Z.W.B., Yi Zheng,
727 Z.Y.X., 2004. Effects of soil conservation measures on erosion rates and crop productivity on
728 subtropical Ultisols in Yunnan Province, China. Agriculture, Ecosystems and Environment
729 104(2), 343-357.
730
731 Bonniwell, E.C., Matisoff, G., Whiting, P.J., 1999. Determining the times and distances of
732 particle transit in a mountain stream using fallout radionuclides. Geomorphology 27, 75-92.
733
734 Bravo-Espinosa, M., Mendoza, M.E., Medina-Orozco, L., Prat, C., Garcia-Oliva, F., Lopez-
735 Granados, E. 2009. Runoff, soil loss, and nutrient depletion under traditional and alternative
736 cropping systems. Land Degradation and Development 20 (6), 640-653.
737

738 Brost, R.A., Fleicher, J., Heimann, M., 1991. Three-dimensional simulation of ^{7}Be in a global
739 climate model. Journal of Geophysical Research 96, 22423-22445.
740
741 Caillet, S., Arpagaus, P., Monna, F., Dominik, J., 2001. Factors controlling ^{7}Be and ^{210}Pb
742 atmospheric deposition as revealed by sampling individual rain vents in the region of Geneva,
743 Switzerland. Journal of Environmental Radioactivity 53, 241-256.
744
745 Ciffroy, P., Reyss, J.L., Siclet, F., 2003. Determination of the residence time of suspended
746 particles in the turbidity maximum of the Loire estuary by ^{7}Be analysis. Estuarine Coastal and
747 Shelf Science 57, 553-568.
748
749 Dedkov, A.P., Moszherin, V.I., 1992. Erosion and sediment yield in mountain regions of the
750 world. Erosion, debris flow and environment in mountain regions. IAHS publication 209, 29-
751 36.
752
753 Descroix, L., González Barrios, J.L., Viramontes, D., Poulenard, J., Anaya, E., Esteves, M.,
754 Estrada, J., 2008. Gully and sheet erosion on subtropical mountain slopes: Their respective
755 roles and the scale effect. Catena 72(3), 325-339.
756
757 Dias, M.I., Prudêncio, M.I., 2008. On the importance of using scandium to normalize
758 geochemical data preceding multivariate analyses applied to archaeometric pottery studies.
759 Microchemical Journal 88, 136-141.
760
761 Dominik, J., Burrus, D., Vernet, J.P., 1987. Transport of the environmental radionuclides in
762 an alpine watershed. Earth and Planetary Science Letters 84, 165-180.

763

764 Duvert, C., Gratiot, N., Evrard, O., Navratil, O., Némery, J., Prat, C., Esteves, M., in press.
765 Drivers of erosion and suspended sediment transport in three contrasted headwater
766 catchments of the Mexican Central Highlands. Geomorphology.

767

768 Etchevers Barra, J.D., Hidalgo Moreno, C., Prat, C., Quantin, P., 2004. Tepetates of Mexico.
769 In: Lal, R. (Ed.), *Encyclopaedia of Soil Science*. Marcel Dekker Inc., New York, pp. 1745-
770 1748.

771

772 FAO, 2006. World Reference Base for Soil Resources 2006. A Framework for International
773 Classification, Correlation and Communication. Vol. 103. FAO, Roma, Italy, 145 pp.

774

775 Gil-García, C., Rigol, A., Vidal, M., 2009. New best estimates for radionuclide solid–liquid
776 distribution coefficients in soils, Part 1: radiostrontium and radiocaesium. Journal of
777 Environmental Radioactivity 100, 690-696.

778

779 Gratiot, N., Duvert, C., Collet, L., Vinson, D., Némery, D., Saenz-Romero, C., 2010.
780 Increase in surface runoff in the central mountains of Mexico: lessons from the past and
781 predictive scenario for the next century. Hydrol. Earth Syst. Sci. 14 (2), 291-300.

782

783 Inbar, M., Tamir, M., Wittenberg, L., 1998. Runoff and erosion processes after a forest fire in
784 Mount Carmel, a Mediterranean area. Geomorphology 24(1), 17-33.

785

786 INEGI, 1985. Síntesis geográfica del Estado de Michoacán. INEGI, Mexico (DF), 316 pp.

787

INEGI, 2006. Conteo de Población y Vivienda 2005, Resultados definitivos. Sistema Nacional de Información Estadística y Geográfica, Mexico City, Mexico.

Jin, Z., Li, F., Cao, J., Wang, S., Yu, J., 2006. Geochemistry of Daihai Lake sediments, Inner Mongolia, north China: implications for provenance, sedimentary sorting, and catchment weathering. Geomorphology 80, 147-163.

Le Cloarec, M.F., Bonté, P., Lefèvre, I., Mouchel, J.M., Colbert, S., 2007. Distribution of ^{7}Be, ^{210}Pb and ^{137}Cs in watersheds of different scales in the Seine River basin: inventories and residence times. Science of the Total Environment 375 (1-3), 125-139.

Le Cloarec, M.F., Bonté, P.H., Lestel, L., Lefèvre, I., Ayrault, S., in press. Sedimentary record of metal contamination in the Seine River during the last century. Physics and Chemistry of the Earth, Parts A/B/C.

López-Granados, E.M., Bocco, G., Mendoza, M.E., 2001. Predicción del cambio de cobertura y uso del suelo, El caso de la ciudad de Morelia, Investigaciones Geográficas, Boletín del Instituto de Geografía, UNAM 45, 56–76, 2001.

Mano, V., Nemery, J., Belleudy, P., Poirel, A., 2009. Assessment of suspended sediment transport in four Alpine watersheds (France): influence of the climatic regime. Hydrological Processes 23, 777-792.

Matisoff, G., Wilson, C.G., Whiting, P.J., 2005. The $^{7}Be/^{210}Pb_{xs}$ ratio as an indicator of suspended sediment age or fraction new sediment in suspension. Earth Surface Processes and Landforms 30, 1191-1201.

Mendoza, M.E., López-Granados, E.M., 2007. Caracterización físico-geográfica de la subcuenca de Cointzio, Michoacán: información básica para el manejo integrado de cuencas. In: Sánchez-Brito, C., Fragoso-Tirado, E., Bravo-Espinoza, M. (Eds.) Bases Metodológicas para el Manejo Integrado de Cuencas Hidrológicas, edited by: Libro Técnico INIFAP.

Meybeck, M., Laroche, L., Dürr, H.H., Syvitski, J.P.M., 2003. Global variability of daily total suspended solids and their fluxes in rivers. Global and Planetary Change 39, 65-93.

Némery, J., Mano, V., Navratil, O., Gratiot, N., Duvert, C., Legout, C., Belleudy, P., Poirel, A., Esteves, M., 2010. Retour d'expérience sur l'utilisation de la turbidité en rivière de montagne. Tech. Sci. Méthodes 1(2), 61-67. (In French).

Nyssen, J., Poesen, J., Moeyersons, J., Deckers, J., Haile, M., Lang, A., 2004. Human impact on the environment in the Ethiopian and Eritrean highlands—a state of the art. Earth-Science Reviews 64(3-4), 273-320.

Owens, P.N., Batalla, R.J., Collins, A.J., Gomez, B., Hicks, D.M., Horowitz, A.J., Kondolf, G.M., Marden, M., Page, M.J., Peacock, D.H., Petticrew, E.L., Salomons, W., Trustrum, N.A., 2005. Fine-grained sediment in river systems: environmental significance and management issues. River Research and Applications 21, 693-717.

836 Poulenard, J., Podwojewski, P., Janeau, J.L., Collinet, J., 2001. Runoff and soil erosion under
837 rainfall simulation of Andisols from the Ecuadorian *Páramo*: effect of tillage and burning.
838 Catena 45(3), 185-207.
839
840 Prosser, I.P., Abernethy, B., 1999. Increased erosion hazard resulting from log-row
841 construction during conversion to plantation forest. Forest Ecology and Management 123 (2-
842 3), 145-155.
843
844 Ramirez-Olvera, M.A., Diaz-Arguero, M., Lopez-Lopez, E., 2004. Planktonic crustacean
845 assemblages in a system of three reservoirs in the Mexican Central Plateau: Seasonal and
846 spatial patterns. Journal of Freshwater Ecology 19, 25-34.
847
848 Reyss, J.L., Schmidt, S., Legeleux, F., Bonté, P., 1995. Large, low background well-type
849 detector for measurements of environmental radioactivity. Nuclear Instruments and Methods
850 A357, 391-397.
851
852 Roldán, A., Caravaca, F., Hernández, M. T., García, C., Sánchez-Brito, C., Velásquez, M.,
853 Tiscareño, M., 2003. No-tillage, crop residue additions, and legume cover cropping effects on
854 soil quality characteristics under maize in Patzcuaro watershed (Mexico). Soil and Tillage
855 Research 72(1), 65-73.
856
857 Salles, C., Poesen, J., Sempere-Torres, D., 2002. Kinetic energy of rain and its functional
858 relationship with intensity. Journal of Hydrology 257 (1-4), 256-270.
859

Sánchez-Chardi, A., Oliveira Ribeiro, C.A., Nadal, J., 2009. Metals in liver and kidneys and the effects of chronic exposure to pyrite mine pollution in the shrew *Crocidura russula* inhabiting the protected wetland of Doñana. Chemosphere 76(3), 387-394.

Sepulveda, A., Schuller, P., Walling, D.E., Castillo, A., 2008. Use of ^{7}Be to document soil erosion associated with a short period of extreme rainfall. Journal of Environmental Radioactivity 99 (1), 35-49.

Servenay, A., Prat, C., 2003. Erosion extension of indurated volcanic soils of Mexico by aerial photographs and remote sensing analysis. Geoderma 117 (3-4), 367-375.

Susperregui, A.S., Gratiot, N., Esteves, M., Prat, C., 2009. A preliminary hydrosedimentary view of the highly turbid, tropical, manmade lake: Cointzio Reservoir (Michoacan, Mexico). Lakes and reservoirs: Research and Management 14, 31-39.

Tamtam, F., Mercier, F., Le Bot, B., Eurin, J., Tuc Dinh, Q., Clément, M., Chevreuil, M., 2008. Occurrence and fate of antibiotics in the Seine River in various hydrological conditions. Science of The Total Environment 393 (1), 84-95.

Urban, J.D., Tachovsky, J.A., Haws, L.C., Wikoff Staskal, D., Harris, M.A., 2009. Assessment of human health risks posed by consumption of fish from the Lower Passaic River, New Jersey. Science of the Total Environment 408 (2), 209-224.

Wang, K., Cornett, R.J., 1993. Distribution coefficients of ^{210}Pb and ^{210}Po in laboratory and natural aquatic systems. Journal of Paleolimnology 9, 179-188.

Wilson, C.G., Matisoff, G., Whiting, P.J., Klarer, D.M., 2005. Transport of fine sediment through a wetland using radionuclide tracers: Old Woman Creek, OH. Journal of Great Lakes Research 31(1), 56-67.

Figure captions

Fig. 1. Location of the monitored subcatchments (Huertitas, Potrerillos, La Cortina) within the Cointzio catchment (outlet located at 19°37'46''N / 101°15'35''W).

Fig. 2. Land uses in the study sites derived from the map drawn by Mendoza and López-Granados (2007).

Fig. 3. Partial view of the Huertitas subcatchment, showing the gully systems, cropland and rangeland (picture taken on 25 June 2009).

Fig. 4. Conceptual sketch of the radionuclide mass-balance model improved by Le Cloarec et al. (2007).

Fig. 5. Relationships between rainfall and radionuclide atmospheric fallout in the Cointzio catchment: (A) Be-7; (B) excess-Pb-210.

910

911 Fig. 6. Suspended sediment age and fraction of new sediment in suspension in the three study

912 sites throughout the 2009 rainy season.

913

914 Fig. 7. Suspended sediment yields from the three study sites and value of the Be-7/excess-Pb-

915 210 ratio throughout the 2009 rainy season.

Figure 1

Fig. 1

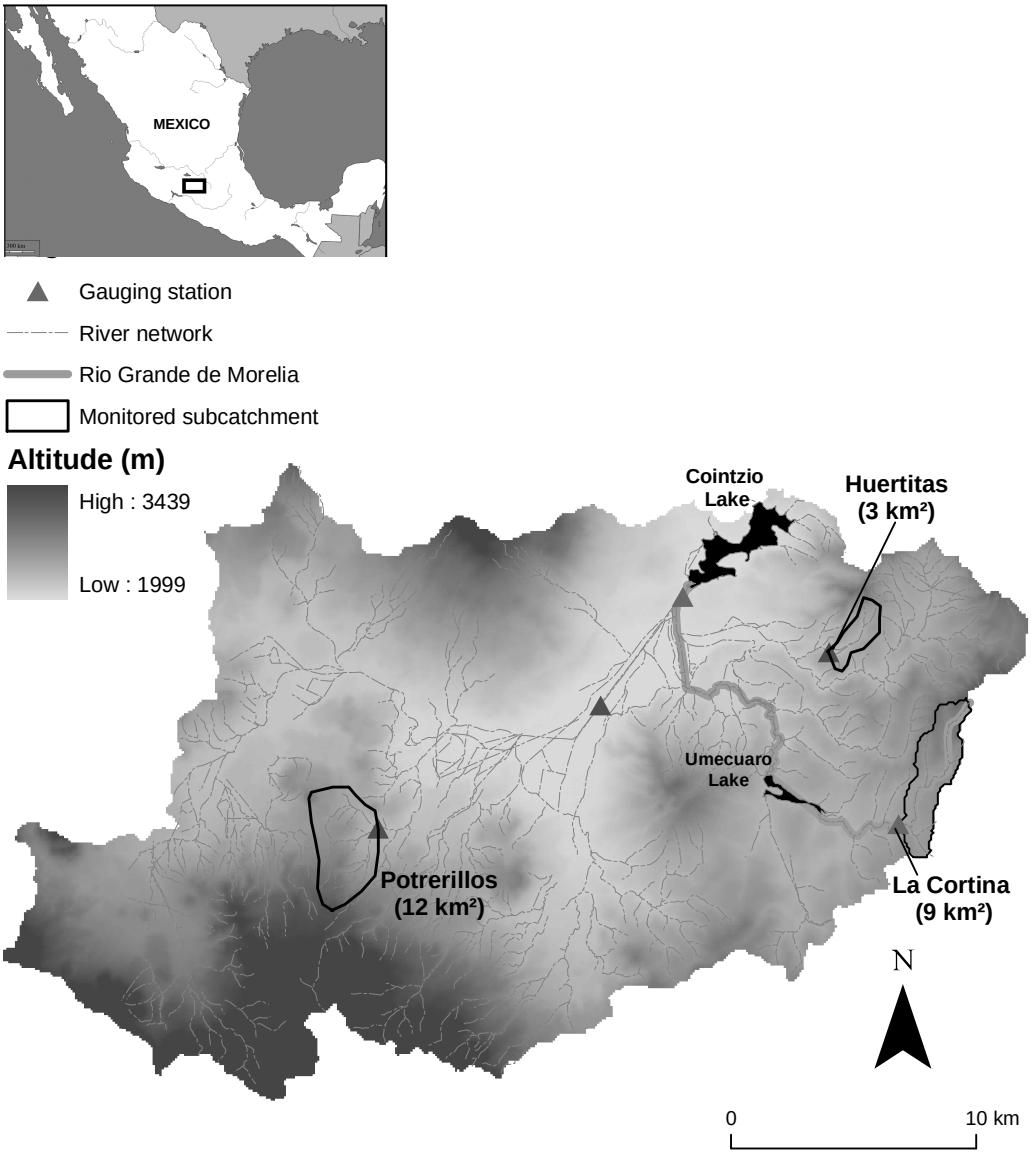

Figure 2

Fig. 2

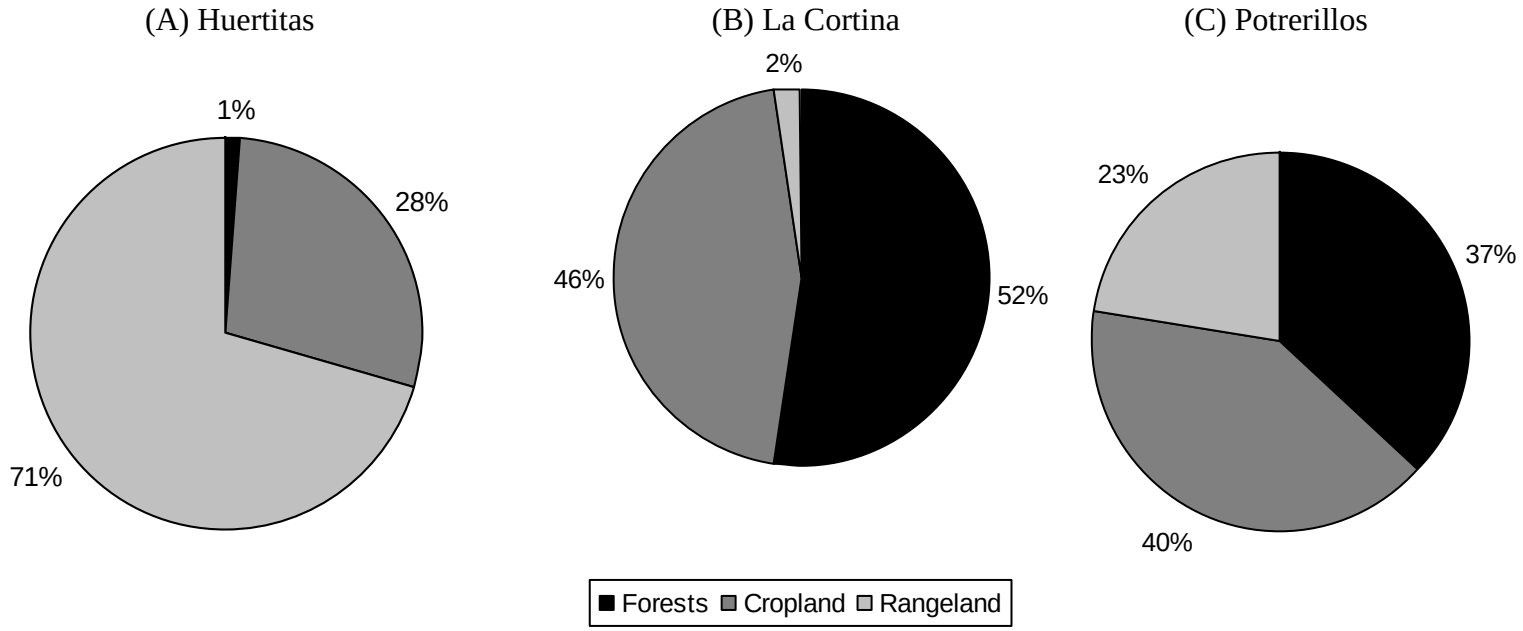

Figure 3

Fig. 3

Figure 4

Fig. 4

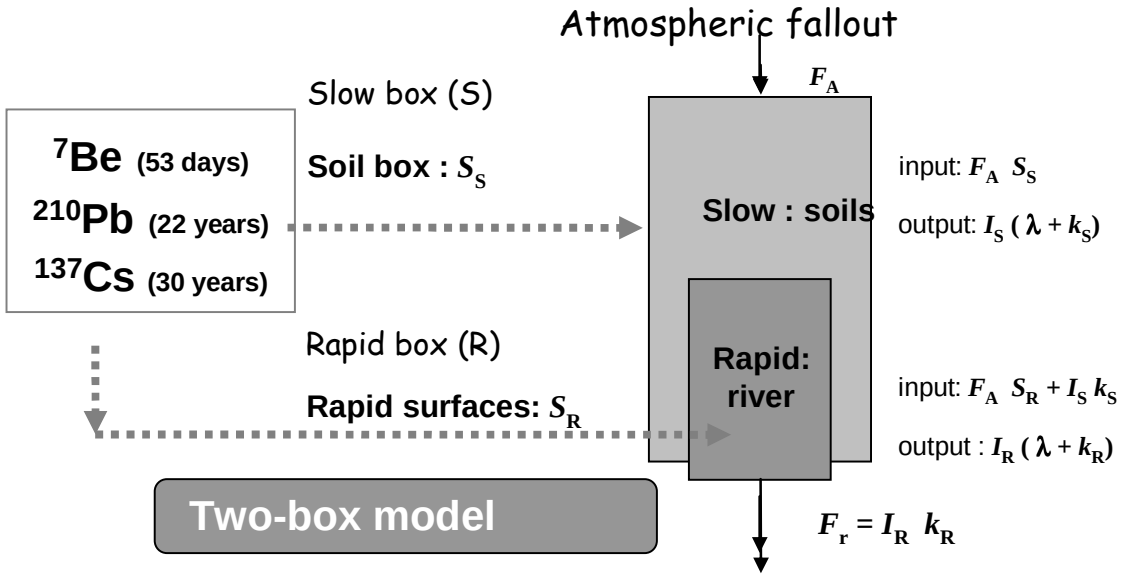

Figure 5

Fig. 5

(A)

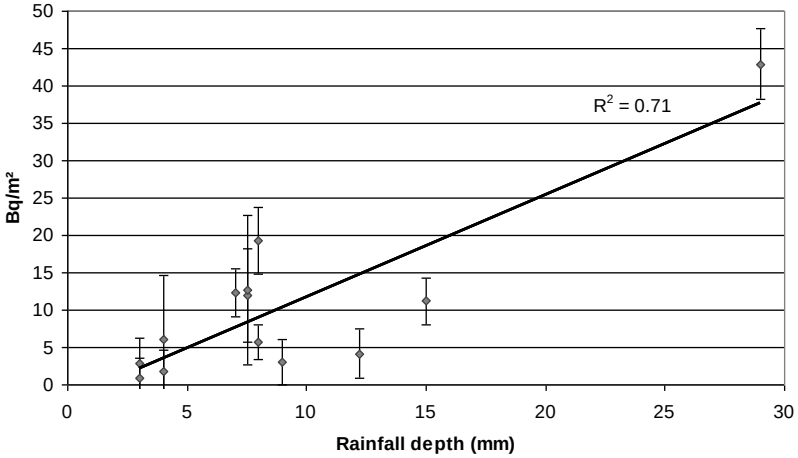

(B)

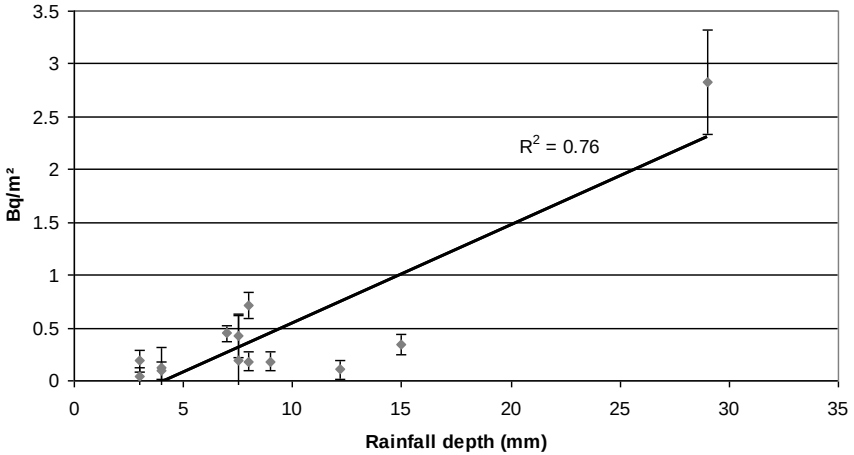

Figure 6

Fig. 6

(A) Huertitas

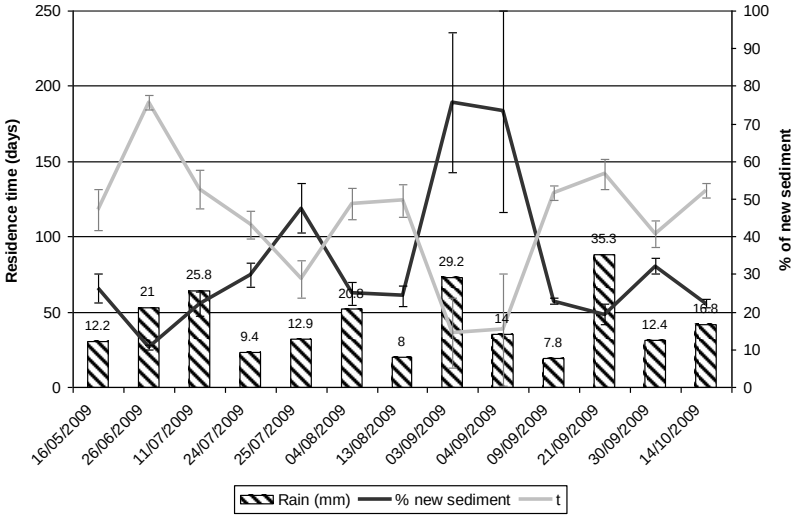

(B) La Cortina

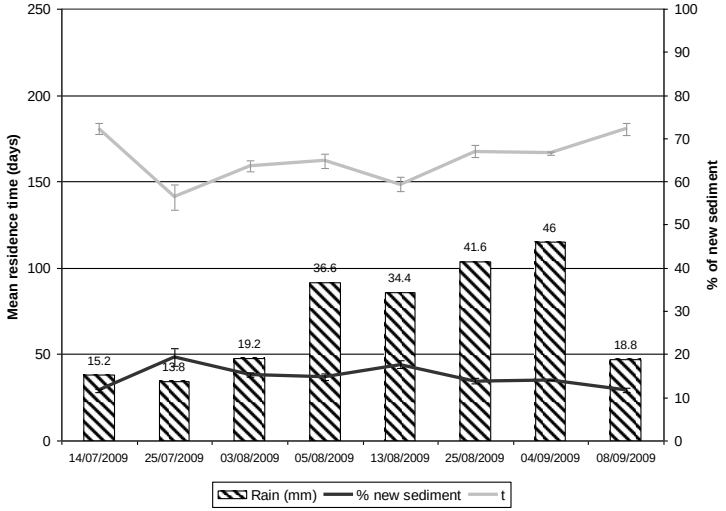

(C) Potrerillos

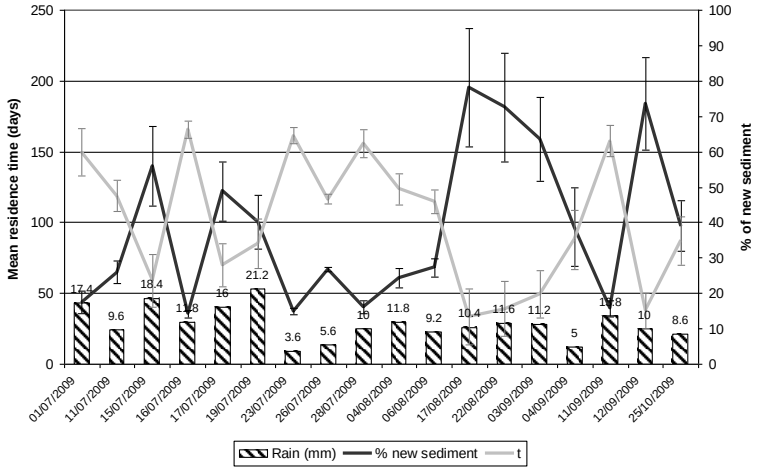

Figure 7

Fig. 7

(A) Huertitas

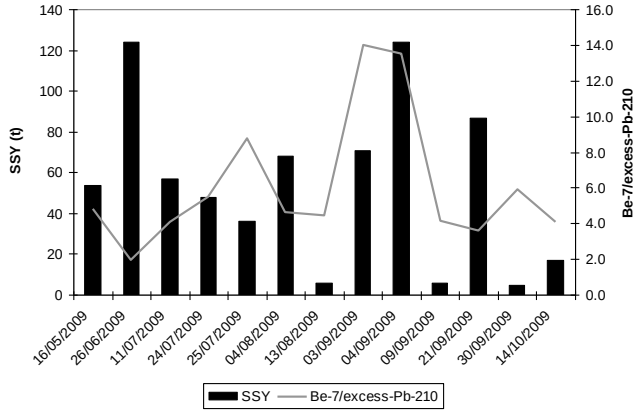

(B) La Cortina

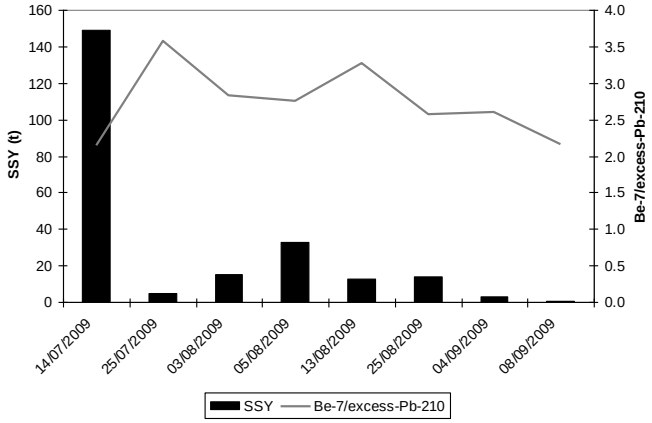

(C) Potrerillos

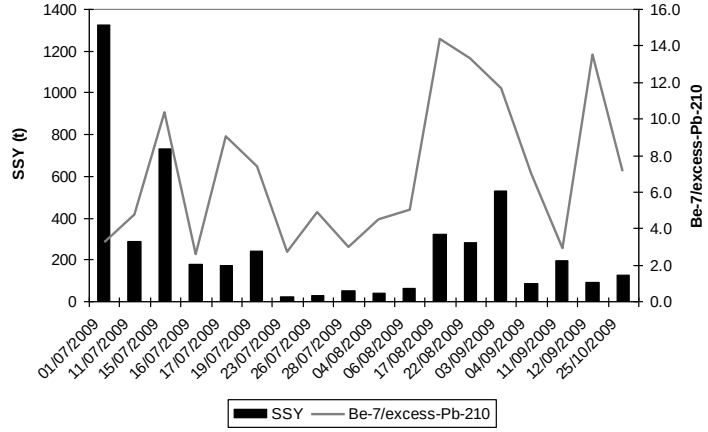

Table 1

Table 1

Altitude, soil, slope, and erosion characteristics of the study sites

Subcatchment	Area (km^2)	Altitude range (m)	Soil types [a]	Slope (% of catchment area)			Severely eroded areas[b]
				0 – 9°	10 – 20°	> 20°	(% of the catchment surface)
Huertitas	3	2150 – 2450	Acrisols (100%)	58%	37%	5%	6
La Cortina	9	2250 – 2700	Andisols (100%)	79%	20%	1%	0
Potrerillos	12	2200 – 2700	Acrisols (60%) Andisols (40%)	71%	28%	1%	1

[a] According to FAO (2006).

[b] Derived from the analysis of aerial photographs.

Table 2

Table 2
Rainfall, runoff, and sediment characteristics of the floods sampled at the outlet of the three study sites in 2009[a]

Event date	Rainfall (mm)	Runoff (mm)	RC (%)	SSY (t)	KE (J m^{-2} mm^{-1})	xs-Pb-210 (Bq kg^{-1})	Cs-137 (Bq kg^{-1})	Be-7 (Bq kg^{-1})	Flood type
(a) Huertitas (n = 13)									
16/05/2009	12.2	0.3	2.5	54	n/a	6 (±1)	0.4 (±0.1)	29 (± 1)	LaP
26/06/2009	21.0	1.9	9.2	124	220	15 (±3)	0.5 (±0.3)	29 (± 4)	SP
11/07/2009	25.8	1.4	5.3	57	263	11 (±3)	0.5 (±0.5)	45 (± 4)	LeP
24/07/2009	9.4	0.8	8.2	48	n/a	13 (±2)	< 0.3	71 (± 4)	LeP
25/07/2009	12.9	0.7	5.4	36	n/a	8 (±2)	< 0.2	70 (± 3)	LeP
04/08/2009	20.8	1.1	5.3	68	206	10 (±2)	0.4 (±0.2)	46 (± 3)	LeP
13/08/2009	8.0	0.2	2.5	6	58	16 (±4)	< 0.4	71 (± 5)	LeP
03/09/2009	29.2	1.2	4.1	71	487	4 (±2)	< 0.1	56 (± 3)	LeP
04/09/2009	14.0	2.0	14.0	124	232	< 3.0	0.3 (±0.1)	27 (± 3)	SP
09/09/2009	7.8	1.0	12.8	6	n/a	18(±4)	< 0.3	75 (± 5)	LeP
21/09/2009	35.3	4.2	11.9	87	180	12 (±3)	< 0.3	43 (± 4)	LeP
30/09/2009	12.4	0.7	5.6	5	310	12 (±4)	0.6 (±0.4)	71 (± 6)	LeP
14/10/2009	16.8	0.8	4.6	17	261	19 (±2)	0.9 (±0.2)	62 (± 4)	LeP
(b) La Cortina (n = 8)									
14/07/2009	15.2	6.1	3.9	149	438	40 (± 4)	2.8 (± 0.3)	86 (± 5)	LaP
25/07/2009	13.8	0.4	0.2	5	272	50 (± 8)	2.5 (± 0.9)	179 (± 15)	LeP
03/08/2009	19.2	0.9	0.5	15	377	55 (± 7)	3.3 (± 0.6)	156 (± 12)	LeP
05/08/2009	36.6	1.6	0.4	33	492	24 (± 3)	2.4 (± 0.3)	66 (± 4)	LeP
13/08/2009	34.4	1.4	0.4	13	347	48 (± 3)	2.0 (± 0.3)	154 (± 6)	SP
25/08/2009	41.6	1.5	0.3	14	386	39 (± 3)	2.0 (± 0.3)	100 (± 4)	LeP
04/09/2009	46.0	0.7	0.2	3	396	45 (± 4)	0.7 (± 0.5)	117 (± 7)	LeP
08/09/2009	18.8	0.8	0.4	1	763	58 (± 7)	3.7 (± 1.6)	125 (± 10)	LeP

Event date	Rainfall (mm)	Runoff (mm)	RC (%)	SSY (t)	KE (J m^{-2} mm^{-1})	xs-Pb-210 (Bq kg^{-1})	Cs-137 (Bq kg^{-1})	Be-7 (Bq kg^{-1})	Flood type
(c) Potrerillos (n = 18)									
01/07/2009	17.4	1.3	9.6	1326	195	5 (± 2)	0.5 (± 0.1)	16 (± 2)	SP
11/07/2009	9.6	1.0	13.1	290	234	8 (± 2)	< 0.2	38 (± 2)	SP
15/07/2009	18.4	1.4	9.6	394	194	< 4	0.3 (± 0.1)	31 (± 2)	SP
16/07/2009	11.8	0.8	8.2	176	158	15 (± 2)	< 0.2	39 (± 3)	SP
17/07/2009	16.0	0.8	6.4	175	223	6 (± 1)	0.3 (± 0.1)	54 (± 2)	SP
19/07/2009	21.2	1.2	7.1	240	463	5 (± 1)	0.3 (± 0.1)	37 (± 2)	SP
23/07/2009	3.6	0.2	7.2	23	94	31 (± 6)	1.1 (± 0.6)	83 (± 9)	SP
26/07/2009	5.6	0.2	4.6	29	149	14 (± 4)	< 0.3	68 (± 5)	SP
28/07/2009	10.0	0.3	3.8	50	146	17 (± 4)	< 0.4	50 (± 4)	SP
04/08/2009	11.8	0.3	3.1	39	164	19 (± 4)	1.0 (± 0.5)	85 (± 7)	LaP
06/08/2009	9.2	0.5	6.4	63	179	16 (± 3)	0.5 (± 0.3)	80 (± 4)	SP
17/08/2009	10.4	1.4	17.8	320	227	< 3	0.2 (± 0.1)	43 (± 2)	LeP
22/08/2009	11.6	1.3	14.6	280	314	< 4	0.3 (± 0.2)	40 (± 2)	SP
03/09/2009	11.2	1.4	16.0	531	161	< 3	0.4 (± 0.1)	35 (± 3)	LeP
04/09/2009	5.0	0.5	13.3	84	205	6 (± 2)	< 0.3	42 (± 4)	SP
11/09/2009	13.8	1.6	14.6	216	403	9 (± 3)	1.2 (± 0.4)	26 (± 5)	LaP
12/09/2009	10.0	0.5	6.1	74	97	< 5	< 0.2	54 (± 4)	SP
25/10/2009	8.6	0.8	9.5	125	64	7 (± 2)	< 0.2	50 (± 3)	SP

[a]RC: runoff coefficient; SSY: suspended sediment yield; KE: kinetic energy; n/a: not available.
Flood type as defined by Duvert et al. (in press). See the text for details.

Table 3

Table 3

Mean atmospheric fluxes of Be-7, Pb-210, and Cs-137 in each subcatchment in 2009

Subcatchment	Area (km^2)	Rainfall (mm)	$F_{a(Be)}$ (GBq d^{-1})	$F_{a(Pb)}$ (GBq d^{-1})	$M_{(Cs)}$ (GBq)
Huertitas	3.0	593	0.008	0.0005	3
La Cortina	9.0	1169	0.068	0.0038	11
Potrerillos	12.0	765	0.059	0.0033	14

Table 4

Table 4

Mean river fluxes of Be-7, Pb-210, and Cs-137 in each subcatchment

Subcatchment	$F_{r\,(Be)}$ (GBq d^{-1})	$F_{r\,(Pb)}$ (GBq d^{-1})	$F_{r\,(Cs)}$ (GBq km^{-2})	$(F_a/F_r)_{(Pb)}$	$(F_a/F_r)_{(Be)}$
Huertitas	1.7×10^{-4}	3.4×10^{-5}	1.8×10^{-6}	14	47
La Cortina	5.1×10^{-5}	1.8×10^{-5}	1.2×10^{-6}	203	1353
Potrerillos	4.2×10^{-4}	5.8×10^{-5}	2.8×10^{-6}	56	139

Table 5

Table 5

Model estimations of the sediment residence times in the river (τ_r) and soil (τ_s) boxes of each subcatchment; proportion of the sub-catchment area covered by the river box (S_r)

Subcatchment	τ_r (d)		τ_s (y)		S_r (%)	
Huertitas	60	(± 40)	5000	(± 1500)	4.5	(± 1.5)
La Cortina	200	(± 70)	23,300	(± 7000)	0.3	(± 0.1)
Potrerillos	50	(± 30)	13,300	(± 4000)	1.5	(± 0.5)

Table 6

Calculated inventories of Be-7, Pb-210, and Cs-137 in the soil boxes of the different subcatchments

Subcatchment	$I_{s\ (Pb)}$ (GBq km^{-2})	$I_{s\ (Cs)}$ (GBq km^{-2})	$I_{s\ (Be)}$ (GBq km^{-2})	$(I_r/I_s)_{(Be)}$
Huertitas	1.7	1.1	0.3	0.132
La Cortina	4.7	1.1	0.6	0.003
Potrerillos	3.1	1.1	0.4	0.008

Table 7

Radionuclide concentrations in representative samples of the different land uses observed in the different subcatchments

	Cs-137 ($Bq\ kg^{-1}$)
Huertitas:	
Gullies	< 0.2
Retreat scarp in grassland	0.8 (± 0.2)
Cropland	2.1 (± 0.3)
La Cortina:	
Woodland	11.9 (± 5.8)
Cropland (avocado)	3.1 (± 0.5)
Cropland (maize)	4.1 (± 0.3)

Potrerillos:	
Grassland	0.6 (± 0.3)
Cropland (maize)	2.2 (± 0.4)